Molecular response to multiple trace-element contamination of the European sardine

Anaïs Beauvieux[1], Jean-Marc Fromentin[1], Claire Saraux[2], Diego Romero[3], Nathan Couffin[2,4], Adrien Brown[2,4], Luisa Metral[1], Fabrice Bertile[2,4], Quentin Schull[1]

1 MARBEC, Univ Montpellier, CNRS, Ifremer, IRD, Sète, France

2 Université de Strasbourg, CNRS, IPHC UMR 7178, F-67000 Strasbourg, France

3 Toxicology Department, Faculty of Veterinary Medicine, University of Murcia, 30100 Murcia, Spain

4 Infrastructure Nationale de Protéomique ProFI, FR2048 CNRS CEA, Strasbourg 67087, France

*Corresponding author
Correspondence: anais.beauvieux@gmail.com

ABSTRACT

In marine ecosystems, the presence of trace elements resulting from anthropogenic activities has raised concerns regarding their potential effects on marine organisms. This study delves into the intricate relationship between trace element contamination and the physiological responses of a key marine species in the Mediterranean Sea: the European sardine. Since 2008, this species has been experiencing a significant crisis in the region, prompting numerous studies to investigate the potential factors behind the dramatic decline in sardines' size, age, and body condition. However, thorough information on chemical contamination by trace elements and its physiological impact on this species was lacking. We found evidence for the accumulation of multiple elements in sardines, with a light East-West contamination gradient within the Gulf of Lions. While macro-physiological parameters (i.e. body condition) were not affected by contamination, pathways involved in cellular organization and response to stress were clearly upregulated, particularly in the liver, but also in muscle. In addition, a global upregulation in processes linked to the immune system, lipid homeostasis and oxidative stress was recorded in the liver. The associated energetic cost may add a substantial burden to sardines that already face multi-factorial constraints. This study also allows to pinpoint biomarkers of exposure and effects that may be important for monitoring Mediterranean sardine's health. The results of this study and particularly the complex changes in protein expression demonstrate the need for future studies to test the concomitant effects of multiple stressors acting simultaneously, including large scale contamination.

Keywords: Cocktail effect, Ecotoxicology, Gulf of Lions, *Sardina pilchardus*, Shotgun proteomic

Introduction

The Mediterranean Sea suffers from high levels of pollution, making it one of the most polluted seas in the world. The sea's semi-enclosed nature contributes to the accumulation of pollutants, exacerbated by significant atmospheric inputs such as Saharan dust events, intense human activities (Bucchia et al. 2015; Pedrotti et al. 2016) and riverine outflows on the continental shelves (Durrieu de Madron et al. 2011). This is also intimately linked to the enhanced ability of pelagic food chains to bioaccumulate chemical elements in oligotrophic seas such as the Mediterranean Sea (Harmelin-Vivien et al. 2009; Chouvelon et al. 2018). Among natural and anthropogenic pollutants, trace elements are present in all environmental compartments. Some metals (e.g., Cu, Fe, Zn) are essential for maintaining the healthy function of the cells of all living organisms, particularly due to their role as components or co-factors of different enzymes (Wood et al., 2011). Nonetheless, such elements can become toxic when they exceed certain concentration thresholds, leading to important detrimental effects on the health of organisms (Plum et al. 2010; Dydak et al. 2011; Asaduzzaman et al. 2017). In addition, non-essential trace/heavy metals, such as Pb, Hg, Cd, As, Ni, can cause several types of pathological damage at very low concentration (Wood et al., 2011). The accumulation of these chemicals can influence enzymatic and metabolic activities, disrupting ion homeostasis, reducing growth and adversely affecting body condition and swimming performances (Hollis et al. 1999; Bervoets and Blust 2003; Bervoets et al. 2005). Metals are in fact inducers of oxidative stress in many animals (including fish), causing imbalances between the production of reactive oxygen species (ROS) (e.g. H_2O_2, $HO^{\cdot}$, O-2, $R^{\cdot}$, ROO) and cell antioxidant activity (Halliwell and Gutteridge 2015). Increased ROS due to overproduction and/or the inability to destroy them may damage DNA structures and therefore alter the expression patterns of important proteins, hormones, enzymes, etc. (Morcillo et al. 2016; Javed et al. 2017). Metal contamination also modifies the expression of proteins (biomarkers) linked to cellular responses to stress and cell detoxification. The use of biomarkers, such as antioxidant enzymes (Pereira et al. 2013; Williams and Yoshida-Honmachi 2013), heat shock proteins (HSPs, Downs et al., 2006) and metallothioneins (Sakuragui et al. 2013; Williams and Yoshida-Honmachi 2013) to monitor metal pollution has been widely accepted in environmental and ecotoxicology programs.

While experimental data under controlled conditions taught us a lot on the molecular and physiological costs of single contaminants (Isani et al., 2009; Souid et al., 2015; Wang et al., 2013), the challenge that ecologists now face is to understand the effects of trace element mixtures. Indeed, wildlife species are continuously and increasingly exposed to a large number of different chemicals at the same time (Heys et al. 2016). Therefore, the ecotoxicological impacts of trace element mixtures are relatively less understood. Even at low concentrations, trace elements mixed in the environment can have a combined toxicological effect (Heys et al. 2016) forming “reactive chemical cocktails” that explain the synergistic effects of the combination of distinct elements (Kaushal et al. 2018). Considering the effects of only one pollutant at a time can therefore lead to misinterpretation of biomarker data (Celander 2011).

The emergence of omics tools has provided a potent means of analyzing complex and integrated responses to contaminants. These tools offer high sensitivity and excellent specificity in studying the molecular changes occurring in organisms (Denslow et al. 2005; Benninghoff 2007). Additionally, high-throughout shotgun proteomics (i.e. the direct and rapid analysis of the entire protein compartment within a complex mixture) provides a unique opportunity to comprehensively examine the expression of thousands of proteins in a specific tissue in a single experiment, using mass spectrometry and bioinformatics techniques instead of traditional biochemical methods (Sanchez et al. 2011; López-Pedrouso et al. 2020). This advance considerably improves our understanding at the protein level and further paves the way for identifying new biomarkers of exposure and effect, which can then be used to develop enhanced monitoring programs to better assess the impacts of pollutants on marine species (Apraiz et al. 2006; Benninghoff 2007).

We applied a quantitative proteomics approach to the European sardine (*Sardina pilchardus*) in the northwestern Mediterranean Sea. This small pelagic fish population has indeed shown a drastic decrease in size and body condition since 2008 (Van Beveren et al. 2014), resulting in a lower value on the stalls, which in turn has led to the collapse of the French small pelagic fish fisheries, which landed less than 200 tons in 2022 against 15,000 tons in the early 2000s (Van Beveren et al., 2016). The hypotheses of top-down control through overfishing or natural predation or epizootic diseases have been refuted (Van

Beveren et al. 2016b, 2017, Queiros et al. 2018). The main hypothesis to explain the observed changes is a modification of the quality and/or quantity of sardine preys (such as copepods) due to major environmental changes, thus limiting fish energy resources (bottom-up control, Brosset et al., 2016; Feuilloley et al. 2020; Saraux et al., 2019). However, little is known about a potential impact of contaminants on Mediterranean sardines, as few ecotoxicological studies have been performed so far on small pelagic fishes in the Gulf of Lions (but see COSTAS project; Tronczynski et al., 2013). In the Mediterranean Sea, surface-enriched concentrations of multiple metals (Co, Cu, Ni and Zn), along with their significant negative correlation with salinity, suggest that concentrations are influenced by the Rhône River plume (e.g. Cossa et al., 2017; Radakovitch et al., 2008). Without a significant tide, the surface extension and main direction of this plume depend on wind and outflow forcing conditions (Broche et al. 1998). In addition, given the sardines' considerable swimming ability, it is uncertain how the spatial distribution of pollutants can overlap that of sardines. Hence, it is crucial to obtain a thorough knowledge of the contamination pressures exerted on small pelagic species such as sardines, as already highlighted by the United Nations Environment Programme UNEP (Baker et al. 2013).

The present study therefore focused on assessing in-situ trace element contamination in juvenile European sardines in the Gulf of Lions (NW Mediterranean Sea) and on the impact of contaminant cocktails on individual health using a proteomic approach. The specific objectives of this work were to: (i) assess the trace element load in wild juvenile sardines and evaluate the spatial variability of this contamination; (ii) investigate the impact of trace element mixtures on the proteome of liver (the main organ implicated in the metabolism of xenobiotics) and red muscle (an organ with high metabolic capacity contributing to a major part of total muscle respiration rate, see Teulier et al., 2019), and identify potential new biomarkers for both tissues that could serve as valuable tools in the long-term monitoring of European sardines' health.

Methods

Study sites and sampling

We collected 105 juvenile sardines in the Gulf of Lions (northwestern Mediterranean Sea, Figure 1). Specimens were collected in June-July 2021 during the yearly PELMED pelagic survey conducted by the French Institute for the Exploitation of the Sea (Bourdeix and Hattab 1985). Trawl locations were dependent on the acoustic echoes detected but covered a wide west-east gradient. Between 3 to 12 sardines per trawl were selected. Sagittal otolith pairs were removed from their otic cavity and read to estimate age. Only age 0 individuals were selected for further analyses. All individuals were measured (total length TL, in mm) and weighed (total mass M, in g). Their body condition was calculated using the Le Cren index Kn as estimated by Brosset et al. (2015), which is commonly used as an indicator of general well-being:

$$Kn = \frac{WW}{0.00607 \times TL^{3.057}}$$

where WW is the total wet mass in g and TL the total length in cm.

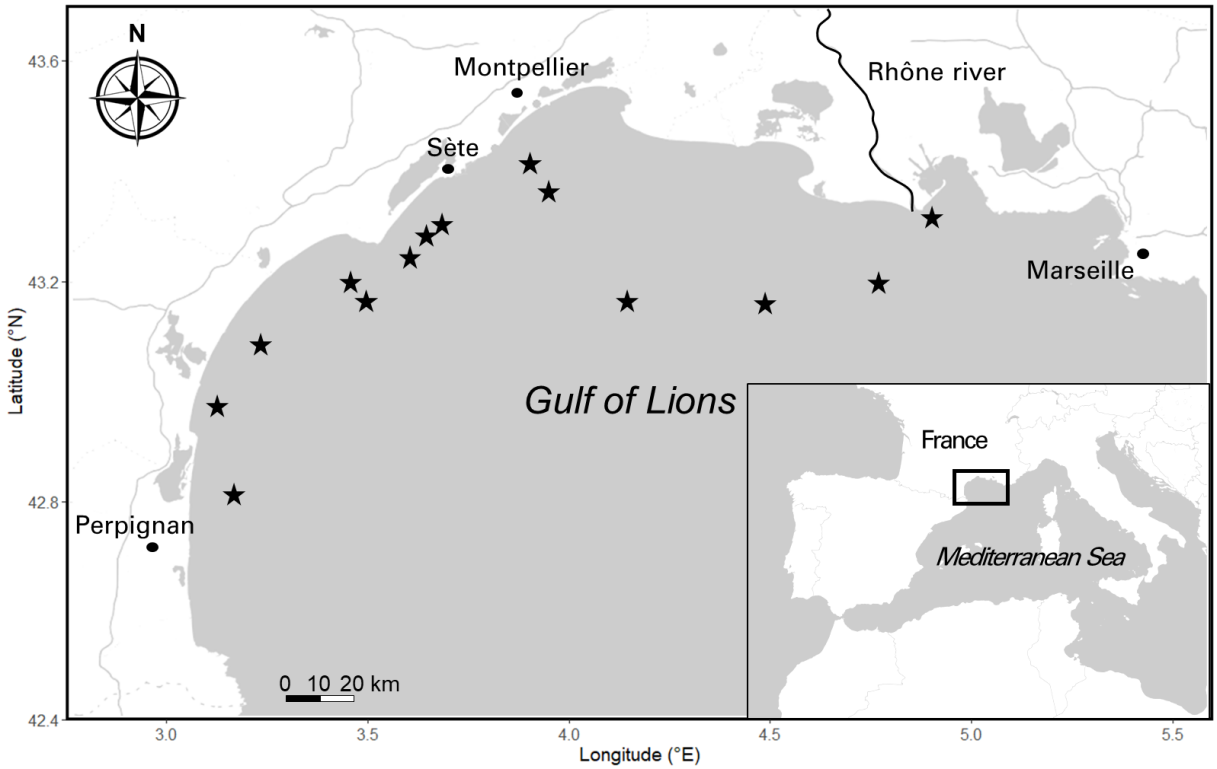

Figure 1. Study area in the Gulf of Lions (northwestern Mediterranean Sea). Pelagic trawling locations for the 105 *S. pilchardus* juveniles in the Gulf are indicated by (★).

Liver and a piece of red muscle were carefully removed to avoid any protein contamination (gloves, a hairnet and a mask were worn by the experimenter and ceramic tools washed with ethanol 96° and MiliQ water), immediately frozen in a dry shipper containing liquid nitrogen (~-190°C, ©CX100 Worthington Industries) on-board and later stored at -80 °C at the lab until proteomics analyses. The white muscle on both sides of the fish was removed using cleansed ceramic tools to avoid any metal contamination and stored at -40°C on-board for the week at sea and then stored at -80°C at the lab until trace element analyses (one side) and lipid content (other side). The red muscle was cleanly separated from the white muscle by scraping the lateral skin stripped from the animal. White muscle samples were taken from the epaxial mass.

Body condition and reserve lipids

Fish body condition was further investigated by determining white muscle reserve lipid content. Lipids were extracted according to the method of Folch et al. (1957) and the content of each class of lipids was measured by chromatography, using a Iatroscan as detailed in Sardenne et al. (2019). Triacylglycerols (TAG), diacylglycerols (DAG as TAG precursors) and free fatty acids (FFA) were grouped together as reserve lipids (Zhol et al. 1995; Tocher 2003; Lloret et al. 2013). The proportions of free fatty acids (FFA) were also checked to ensure that the lipids had not been degraded during sample storage. Here, the proportions were 0.02% on average (only one sample exhibited a concentration in FFA, whereas all the others showed no presence of FFA), significantly below the 25% limit recommended by Parrish (1988).

Trace-element analysis

All samples were lyophilized using a freeze dryer (®Leybold, Cologne, Germany). For aluminium (Al), arsenic (As), beryllium (Be), bismuth (Bi), cadmium (Cd), chromium (Cr), copper (Cu), lithium (Li), nickel (Ni), lead (Pb), rubidium (Rb), antimony (Sb), strontium (Sr), titanium (Ti), thallium (Tl) and zinc (Zn) determination, the samples underwent a pre-treatment process where 0.5 grams of each muscle sample were subjected to acid digestion using 4 mL of HNO3 (69%) and 1 mL of H2O2 (33%) in special Teflon reaction tubes within a microwave digestion system (UltraClave-Microwave Milestone®) for 20 minutes at 220 °C, and then diluted to 10 mL with double deionized water (Milli-Q). Samples were analyzed using

inductively coupled plasma optical emission spectrometry (ICP-OES, ICAP 6500 Duo, Thermo) to determine the levels of this elements. The detection limit was 0.001 mg/kg. Each sample was read in duplicate and averaged. Based on UNE-EN ISO reference 11885, multi-element calibration standards (SCP Science, in 4% nitric acid) were assembled with different concentrations of inorganic elements. For calibration, see (Romero et al., 2020).

Total mercury (Hg) content was measured using an atomic absorption spectrometer AMA254 Advanced Mercury Analyzer (Leco) without pre-treating or pre-concentrating the samples (wavelength = 253.65 nm, detection limit (DL) = 0.003 µg.g-1). The recovery rate for reference materials (Mercury ICP Standard 1000 mg L−1 Hg, Merck) was above 95%.

Quantitative proteomic analysis

In the following proteomic approach, we opted to analyze a subset of 29 individuals who exhibited the most distinct contamination profiles. This selection process involved assigning ranks to sardines based on the level of each contaminant detected. The ranking ranged from 1 (indicating the lowest contamination level) to 105 (representing the highest contamination level). The individuals were then selected based on the total sum of these ranks. Consequently, we identified two groups, one comprising 14 sardines with the lowest contamination levels, and the other consisting of 15 sardines with the highest contamination levels (see Statistical analysis section for further details on individuals'' selection). Proteomic analyses of liver and red muscle were conducted as two separate experiments. The process of sample preparation, nanoLC-MS/MS analysis, and mass spectrometry data analysis is described in detail in ESM1. The procedure involved protein extraction and electrophoresis using SDS-PAGE, followed by in-gel digestion with trypsin (Promega, Madison, WI, USA). The resulting peptides were extracted and analyzed using a nanoUPLC-system (nano-Acquity, Waters, Milford, MA, USA) coupled to a quadrupole-Orbitrap hybrid mass spectrometer (Q-Exactive HF-X, Thermo Scientific, San Jose, CA, USA), controlled by XCalibur software (v4.0.27.9; Thermo Fisher Scientific). The Q-Exactive HF-X was operated using a data-dependent acquisition (DDA) strategy by selecting the Top-20 most intense ions in MS1 for fragmentation in MS2. MS raw data processing was performed in MaxQuant (v2.0.3.1) (Cox et al., 2014), using Andromeda algorithm to search peaklists against a protein database containing protein sequences from a home-made annotation of the genome of Sardina pilchardus (TaxID: 27697; Genbank assembly accession: GCA_003604335.1; Assembly Name: UP_Spi). Only the proteins identified with at least two peptides were retained. Protein quantification was performed using unique peptides only via the MaxLFQ option implemented in MaxQuant (Cox et al., 2014). The mass spectrometry proteomics data have been deposited to the ProteomeXchange Consortium via the PRIDE (Perez-Riverol et al., 2019) partner repository with the dataset identifiers PXD037276 (liver) and PXD037313 (red muscle). QC-related measurements indicated stable performances of the analysis system all along the two experiments, with median coefficients of variation (CV) of 0.47% (liver) and 0.56% (red muscle) for retention times of iRT peptides over all injections. Median CVs of only 10.9% (liver) and 13.8% (red muscle) were obtained for LFQ values of the proteins quantified from the repeated injections of reference samples.

Protein functional annotation

To analyse our proteomic data from a functional point of view, we examined the functional annotations of proteins listed by the AMIGO consortium (Gene Ontology, GO; http://geneontology.org/). However, only one *S. pilchardus* protein is annotated in GO databases. We therefore took advantage of the crucial evolutionary position of the spotted gar (*Lepisosteus oculatus*) between teleost fishes and humans, which creates a very valuable bridge between their genomes (Braasch et al. 2016), and of the fact that gar proteins are well annotated in GO databases. We began by searching L. oculatus sequences (UniprotKB, 22,463 protein entries; September 2022) for proteins homologous to *S. pilchardus* proteins using BLAST searches (FASTA v36.1.4 program; downloaded from http://fasta.bioch.virginia.edu/fasta_www2/fasta_down.shtml), and only the top BLAST hit for each protein was retained. From L. oculatus protein sequences, the same strategy was employed to search for human homologous proteins (TaxID: 9606; Reference proteome accesed in September 2022). The relevance of the match between homologous proteins was checked manually and only 57 of 2505 and 22

of 1112 matches (liver and red muscle, respectively) could not be validated. An automatic extraction of GO annotations was then performed using the MSDA software (Carapito et al. 2014).

Statistical analyses

All statistical analyses were performed with the statistical open source R software v.4.1.1 ((R Core Team, 2021). Element concentrations below Limit Of Detection (LOD, 0.001 mg/kg) were set to "LOD⁄" √("2") as suggested by Verbovsek (2011) as the best substitution method.

Analyses comparing inorganic contamination patterns included only metals that were detected in at least 50% of individuals out of the 105 collected. In order to consider possible relationships between contamination and fish body size, we used a linear model (LM) between each contaminant concentration and the individual total length. Normality and homoscedasticity of the residuals were verified using the Shapiro's and Levene's tests, respectively. When distribution of the residuals did not follow a normal distribution, a log transformation was applied prior to model fitting. If necessary ($P<0.05$), size-corrected contaminant was defined as back-transformed residuals of the regression model.

To investigate relationships between contaminants and to evaluate a possible influence of the Rhône River on trace element loads in sardines within the Gulf of Lions, we performed a Principal Component Analysis (PCA) on scaled size-corrected contaminant concentrations of the 105 individuals and projected distance from the Rhône River on the PCA. We also assessed spearman correlation between the three first principal components (PCs) and the distance of the individuals from the Rhône River delta. To evaluate a potential effect of inorganic contamination on individual's condition, we also performed LMs between the first three PCs and body condition and reserve lipids.

A second PCA approach was performed, using the 29 individuals selected for proteomic analysis as objects only, while the descriptors were scaled size-corrected contaminant concentrations. The aim of this analysis was to summarize all the information to investigate the relationships between contaminants and individual proteomes. PCA axes (PC1, PC2, PC3) were retained as principal components reflecting contaminant mixture 1, mixture 2, mixture 3 and used in further analyses.

Prior to statistical analyses, the proteomic datasets (liver and red muscle) were filtered to keep only proteins that were expressed in at least 70% of individuals in each contamination group (common threshold used in existing literature (Quque et al., 2023; Wang et al., 2020) leaving 2115 (out of 2505) and 913 (out of 1112) expressed proteins in the liver and red muscle, respectively. Three and one individuals were removed due to a high number of missing values for liver and muscle proteome analysis, respectively (supported by the missing value heatmap and proteomic clustering isolation of these individuals). Remaining missing values were imputed for each contamination group based on random forest method (Jin et al., 2021; Kokla et al., 2019). Previous studies have shown that this method exhibits strong performance and is particularly well-suited for label-free proteomic studies, where the underlying reasons for missing data are not fully understood (Jin et al., 2021; Kokla et al., 2019). A log 2 transformation was used to normalize the protein intensities.

Co-expression network and enrichment analysis

Gene co-expression network and hubproteins identification

Weighted gene co-expression network analysis implemented in the WGCNA R package (Langfelder and Horvath 2008) was used for both tissues (liver and red muscle) to identify groups, or modules, of proteins whose expression significantly correlates with inorganic contamination in white muscle. First, an adjacency matrix for all pairs of proteins was constructed using the Spearman correlation raised to the power (beta) of seven and six to approximate a scale-free network for liver and red muscle, respectively (Langfelder and Horvath 2008). The adjacency matrix was then transformed into a topological overlap dissimilarity matrix and a combination of hierarchical clustering and a dynamic tree-cutting algorithm were used to first define and then merge co-expressed modules of proteins. Proteins outside any module (indicating low co-expression) were gathered in a grey module. The module's eigengene (i.e. first module eigenvector: first axis of a principal component analysis conducted on the expression of all module proteins) summarizes the expression of all proteins in that module. Then, we investigated whether the eigengene of the modules was correlated with each contaminant mixture (identified through the PCA analysis, see above), using spearman correlation. Modules with a significant ($P < 0.05$) correlation and at least $R \geq 0.4$ were retained for further analysis (only the grey module

(indicating low co-expression) for muscle presented a significant correlation below 0.4). Positive and negative relationships reflect the up- and down-regulation of the module with an increasing concentration of a contaminant mixture, respectively. To explore the functional and physiological mechanisms associated with each module, we then performed functional enrichment analyses.

Functional enrichment analysis and pathway network

For both tissues, enrichment analysis (biological process and cellular component) of the proteins constituting each module was performed using Fisher's exact test using the '*GO_MWU*' package particularly suitable for non-model organisms (https://github.com/z0on/GO_MWU) (Dixon et al. 2015). It allows to determine the functional significance of the identified modules. Enriched GO terms are displayed in a dendrogram plot with distances between terms reflecting the number of shared proteins. Additionally, we assessed the Spearman correlation between each protein and the contamination mixtures (PCA axes) to infer "gene significance" (GS). Focusing on the top 10 enriched biological process terms (GO terms), these GS relationships were compiled within a circle plot for each enriched pathway of the module. These plots highlight the up- or down-regulation of the proteins and pathways in response to the contaminant mixtures.

Network visualization

ClueGO was used to illustrate overrepresented Gene Ontology terms. ClueGO is a Cytoscape plug-in that visualizes the non-redundant biological terms for large numbers of proteins and integrates the GO terms to create a GO/pathway network (Bindea et al. 2009). A network for each tissue was made in order to visualize the pathways impacted by the three contamination mixtures.

Hubproteins identification

For each module, GS was correlated with module membership (MM; spearman correlation of protein intensity versus the module eigengene) to identify proteins showing the highest degree of connectivity within a module and with the considered contaminant mixture (hubproteins). The top 5 proteins with simultaneously the highest MM and GS (rank sum) were selected as hubproteins in each module. Due to their central position in the network, hubproteins are expected to play important biological roles within their module and are considered as potential biomarkers.

Functional Comparison between tissues

For each contamination mixture, the similarity of the functional response between tissues was compared by plotting their respective GO term delta ranks against each other. GO term delta ranks correspond to the difference between the mean ranks based on the GS of the proteins the GO term contains *vs* the mean ranks of all the protein not included. Positive and negative delta ranks indicate that the GO term tends to be regulated upwards or downwards, respectively. For a given pathway, the strength of the relationship reflects the similarity of the enrichment between liver and red muscle. It is important to note that these plots do not represent a formal statistical test, as the data points (gene ontology categories) are not independent. Indeed, they often encompass overlapping sets of proteins, nonetheless it allows identifying functional similarity or dissimilarity between functional enrichments.

Results

Trace-element burden across Gulf of Lions

Thirteen trace elements (Al, As, Cu, Cr, Hg, Li, Ni, Pb, Rb, Sr, Ti, Tl and Zn, ESM2) were retained after selection of contaminants detected (>LOD) in at least 50% of individuals (i.e. 53 individuals). Only three elements (Pb, Rb and Tl) exhibited a significant relationship with fish length and were size-corrected. While Tl displayed a negative relationship with length (R^2 = 0.16, P<0.001), Pb and Rb had a positive association (R^2 = 0.10, P=0.009 and R^2 = 0.09, P=0.001 respectively).

Considering the 105 sardines sampled across the Gulf of Lions within the same PCA, the first three principal components explained 24.2%, 15.3% and 12.8%, respectively (around 52% in total, ESM3a and

Figure 2). The main contributing variables for the first axis (PC1) were Zn, Sr, Rb, Cu, Pb and As, which all displayed positive contributions (ESM3b and Figure 2). Ni, Cr were positively related to PC2 while, to a lesser extent, Tl was negatively loaded (ESM3c and Figure 2). Ti and Al were negatively loaded along the third axis in opposition to Cr, Ni, Tl and Li (ESM3d and Figure 2). Highlighting the distance of the various sampling sites to the mouth of the Rhône River within the same PCA showed a slight east-west contamination gradient (Figure 2). PC1 and PC2 were negatively correlated with the distance from the Rhone river, albeit slightly above significance levels (ESM4). Nonetheless, there was considerable inter-individual variability in trace element contamination, which probably blurred this East-West gradient (ESM4). The three first PCs displayed no significant correlation with individuals' body condition (P=0.47, P=0.18 and P=0.57 for PC1, PC2 and PC3 respectively), nor with the reserve lipid content (P=0.55, P=0.66 and P=0.79 for PC1, PC2 and PC3 respectively).

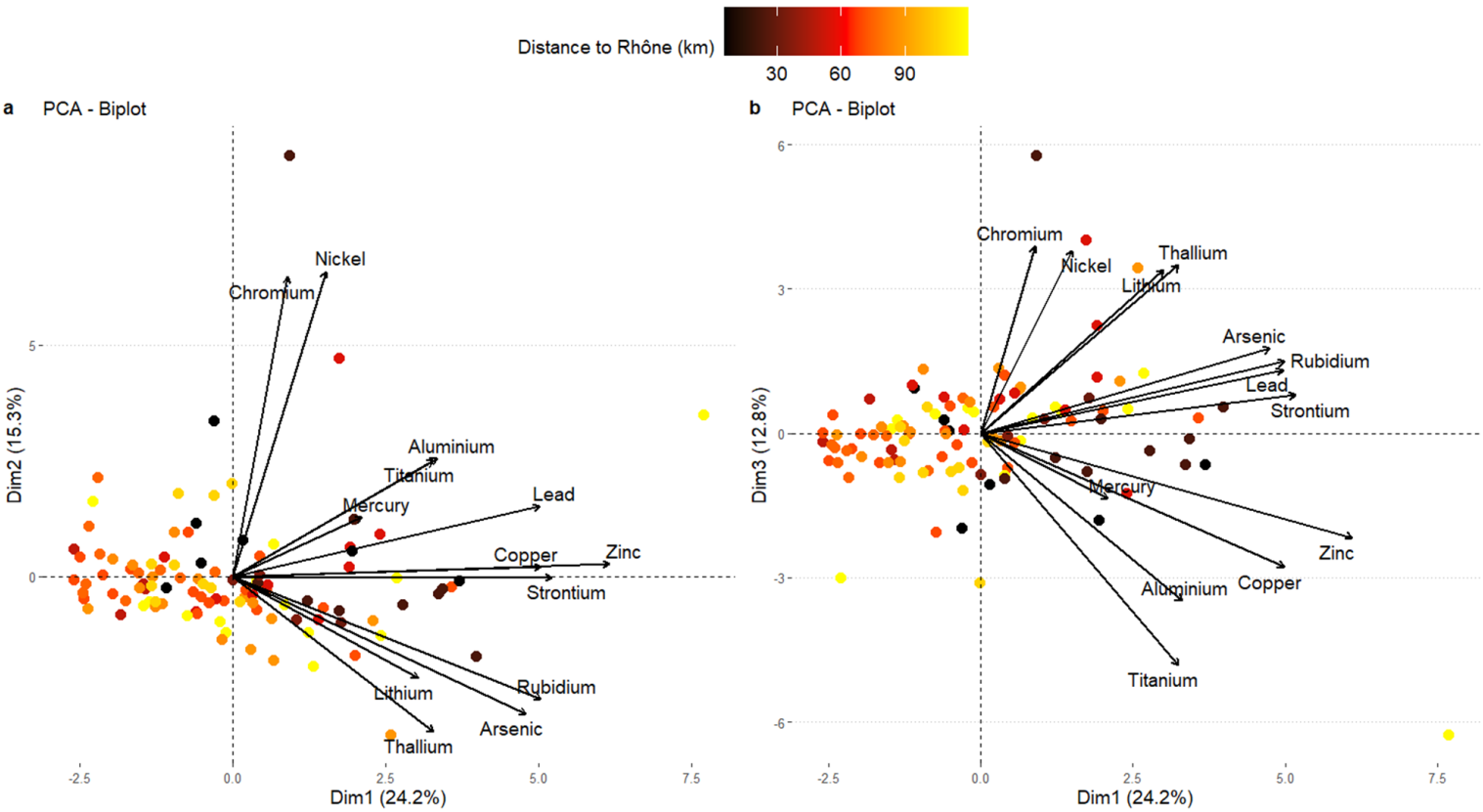

Figure 2. Biplot of PC1 vs PC2 (a) and PC1 vs PC3 (b) of the PCA built with size-corrected level of trace elements present in the 105 individuals sampled across the Gulf of Lionss. Each point represents an individual. Colour gradient indicates the distance from the Rhone river.

Regarding the second PCA performed on the 29 individuals selected for proteomic analysis, the first three principal components displayed 33.3%, 16.9% and 13.6% of the total variance, respectively (around 64% in total, Figure 3 and ESM5). All 13 contaminants loaded positively on PC1 with 8 of them contributing strongly. Further, PC1 clearly separated the 2 groups of individuals previously selected (high contamination *vs* low contamination). Therefore, PC1 was used as a proxy for general inorganic contamination level, which allows to work along a contamination gradient instead of categorical contaminations. PC2 was mostly determined by a strong positive contribution of Ni and Cr, while PC3 was determined by a strong positive contribution of Ti and Al and marginally by a negative contribution of Li. The three PCs independently identified contaminant mixtures, which are listed in Table 1. We next used proteomics to investigate the potential impact of these three contaminant mixtures on the health of the Mediterranean sardine population.

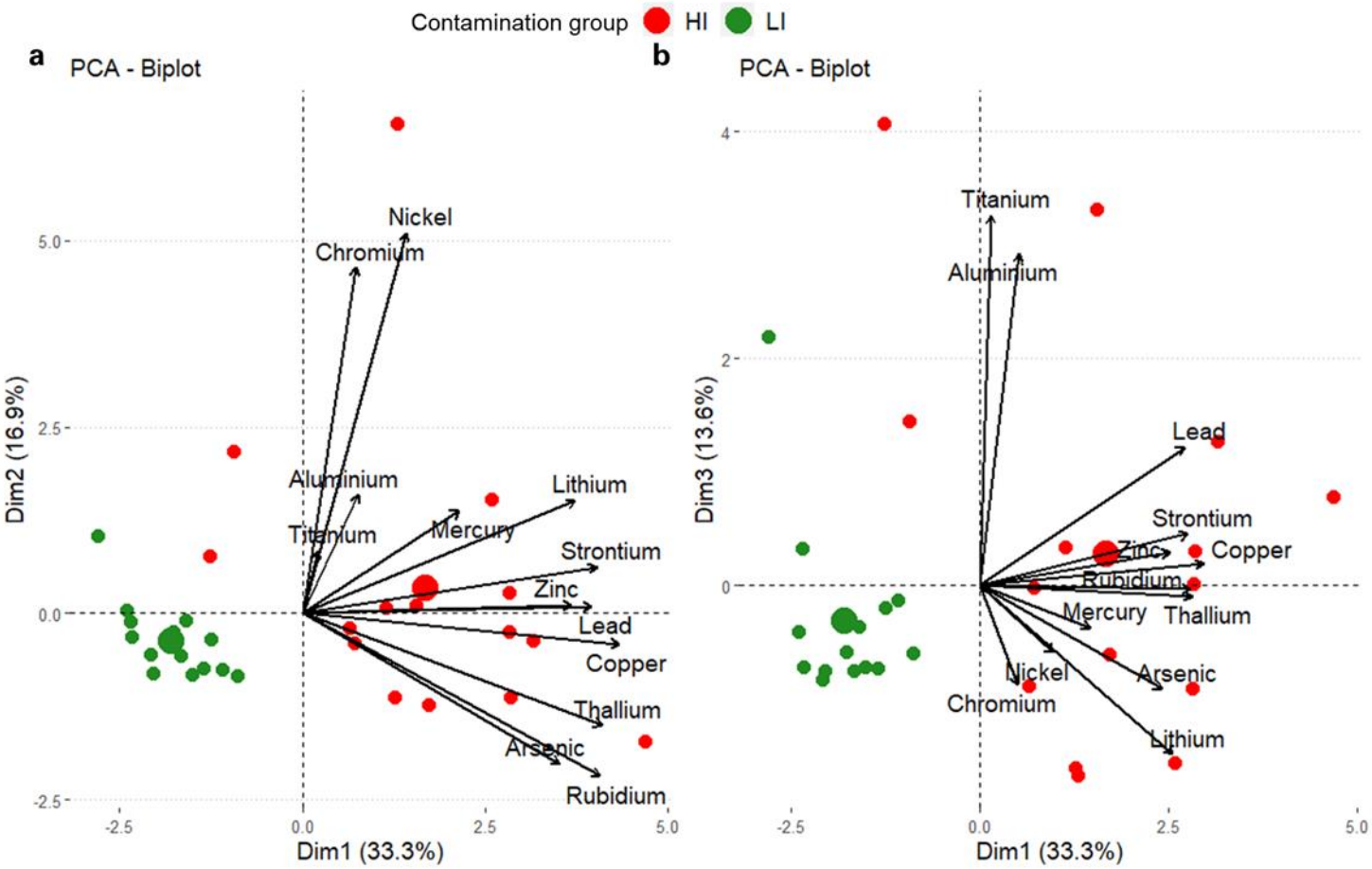

Figure 3. Biplot of PC1 vs PC2 (a) and PC1 vs PC3 (b) of the PCA built with level of inorganic contaminants present in the 29 individuals selected for proteomic analysis. Each point represents an individual. Colours indicate contamination level of individuals (HI: High contamination and LI: Low contamination). The larger circles represent the barycenter of the individuals for a given group.

Table 1. Main variables that contribute to the first three principal components of the PCA on the 29 individuals selected for proteomic analysis. Each PC represents a contaminant mixture.

Mixture 1 - PC1		Mixture 2 - PC2		Mixture 3 - PC3	
-	+	-	+	-	+
none	Cu, Tl, Rb, Sr, Pb, Li, Zn, As	none	Ni, Cr	Li	Ti, Al

Physiological response to inorganic contamination

Using a co-expression network analysis, we focused on the impact of metal contamination at the proteome level on two key organs in fish (the liver and red muscle).

Liver proteome

We detected 9 distinct modules (WGCNA analysis) containing a total of 2115 proteins. We then investigated the relationship between expression modules and the three metal contamination mixtures to assess the potential health effects of inorganic contaminant exposure. Both mixtures 1 and 3 displayed significant positive correlations ($P<0.05$) with the same two co-expressed modules (turquoise and yellow, Figure 4), reflecting a general overexpression of proteins within these 2 modules when mixtures 1 and 3 increased in concentration. Mixture 2 did not display any relationship with any of the co-expressed modules.

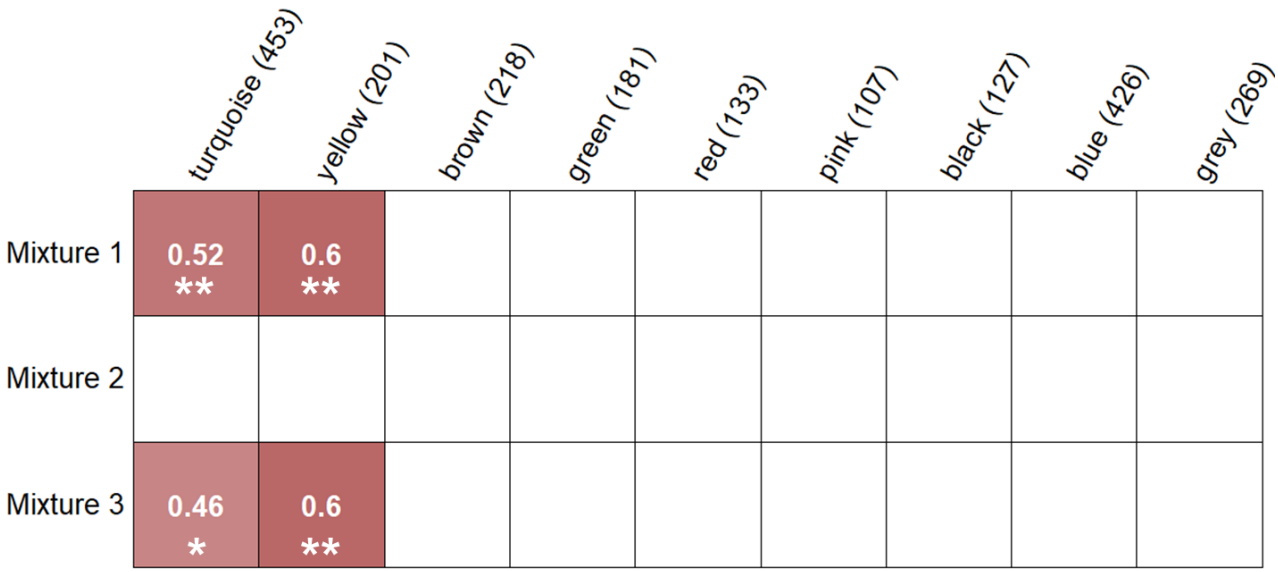

Figure 4. Correlations between module eigengenes (columns) and trace element mixtures (rows) for liver proteome. Values in brackets with module names indicate the number of proteins belonging to each module. Values in the cells are Spearman's correlation coefficients. Blank cells indicate non-significant correlation (P>0.05). *: P<0.05, **: P<0.01

The positive correlation of the turquoise module with mixture 1 (PC1, r = 0.52, P<0.01) and mixture 3 (PC3, r = 0.46, P<0.05) involved an overall upregulation of 170 GO terms (FDR<0.01), mainly involved in anatomical structure and development (e.g., epithelial cell development (GO:0002064), regulation of anatomical structure size (GO:0090066)), response to stimulus/stress (e.g. defense response (GO:0006952), cellular response to DNA damage stimulus (GO:0006974)), protein metabolism (e.g. positive regulation of gene expression (GO:0010628), regulation of protein polymerization), transport and cellular organization (e.g. cell development, regulation of cytoskeleton organization) and cell cycle process (spindle organization, cell cycle process, Figure 5 and ESM6a). Proteins from the turquoise module were part of multiple subcellular compartments, such as the nuclear periphery, endocytic vesicles, immunological synapses and the cytoskeleton (ESM6b). The positive correlation of the yellow module with mixture 1 (P<0.001) displayed a significant enrichment in 71 pathways mainly related to the immune system, the metabolism of lipids and lipoproteins and transport (Figure 5 and ESM7a). Most of these pathways were upregulated in response to an increase in mixture 1 (i.e. Cu, Rb, Sr, Tl, Zn, Li, Pb and As). As for the cellular component analysis, proteins were mainly located in lumens (vesicle, endoplasmic, endocytic) and were subunits of protein complexes (protein-lipid complex, hemoglobin complex, ESM7b).

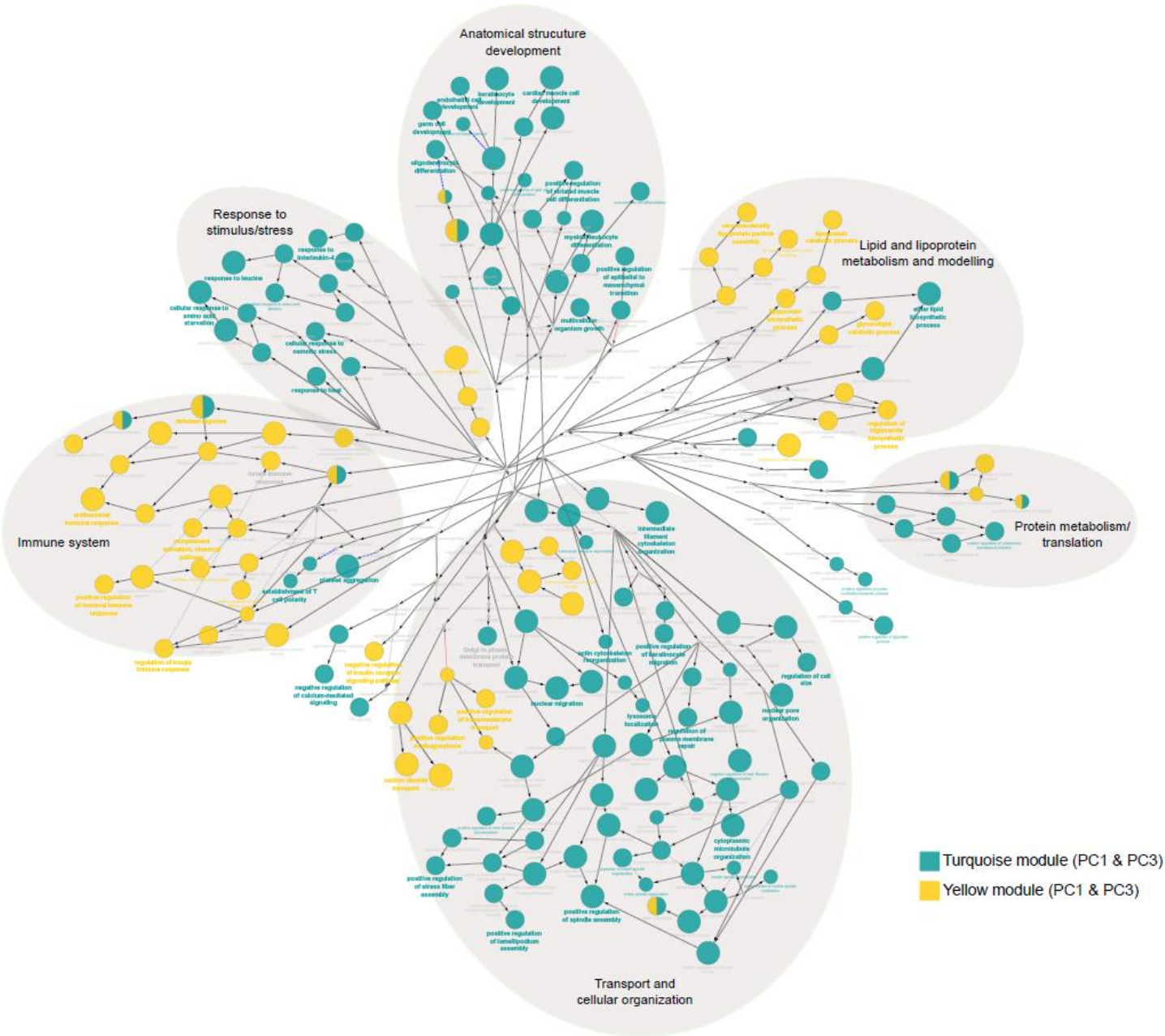

Figure 5. Significant GO terms (FDR <0.001) and ontological relationships in the liver. Colored circle size reflects the level of FDR-adjusted statistical significance. Terms enriched in the same module were grouped and presented in the same color. Each leading term, which has the highest significance, is indicated by bold font. Biological processes were grouped in larger pathways (large grey circles).

To identify potential biomarkers, hubproteins (top 5 proteins with the highest GS and MM) were selected for each module (see Table 2). For the turquoise module, hubproteins were mainly implicated in protein or lipid transport (Table 2). Interestingly, one of them, the Serine/threonine- protein kinase mTOR, was involved in multiple pathways such as cell development, cell structure and metabolism. Potential biomarkers for the yellow module included 2 apolipoproteins with one presenting antioxidant activity (i.e., the Apolipoprotein A-IV). The three other hubproteins were involved in diverse pathways such as protein synthesis with the eukaryotic translation initiation factor 2 subunit 3, cytoskeleton and protein transport with the spectrin beta chain and the DnaJ homolog subfamily C member 13 which is not only implicated in protein transport but also exhibits chaperon function.

Table 2. Top 5 hubproteins selected for each co-expression module in the liver proteome. The name and UniprotKB ID are indicated for each of them as well as their main functions, their module, their expression pattern (up or down-regulation), contaminant mixture they correlate with and the module membership

Name	UniprotKB ID	Module	Main function	Expression pattern	Principal Component	Module membership
Apolipoprotein B-100 isoform 3	APOB	turquoise	Lipid transport and metabolism	↑ up	PC1 and PC3	0.83
Serine/threonine-protein kinase mTOR	MTOR	turquoise	Cell growth, Cell cycle progression, Metabolism, Cellular structure	↑ up	PC1 and PC3	0.81
Cytoplasmic dynein 1 heavy chain 1 isoform 5	DYNC1H1	turquoise	Intracellular motility: cell cycle and transport	↑ up	PC1 and PC3	0.78
U5 small nuclear ribonucleoprotein 200 kDa helicase	SNRNP200	turquoise	mRNA processing/splicing	↑ up	PC1 and PC3	0.89
Cytoplasmic dynein 1 heavy chain 1 isoform 2	DYNC1H1	turquoise	Intracellular motility: cell cycle and transport	↑ up	PC1 and PC3	0.80
Apolipoprotein A-IV	APOA4	yellow	Lipid transport and metabolism, Antioxidant capacity	↑ up	PC1 and PC3	0.88
Apolipoprotein B-100 isoform 1	APOB	yellow	Lipid transport and metabolism	↑ up	PC1 and PC3	0.79
Eukaryotic translation initiation factor 2 subunit 3	EIF2S3	yellow	Translation	↓ down	PC1 and PC3	-0.77
Spectrin beta chain, non-erythrocytic 1	SPTBN1	yellow	Cellular structure, Protein transport/localization	↑ up	PC1 and PC3	0.84
DnaJ homolog subfamily C member 13	DNAJC13	yellow	Chaperone, Protein transport	↑ up	PC1 and PC3	0.88

Muscle proteome

Four modules, namely blue (372 proteins), brown (119 proteins), turquoise (398 proteins) and grey (24 proteins), were obtained from the WGCNA analysis of the red muscle proteome.

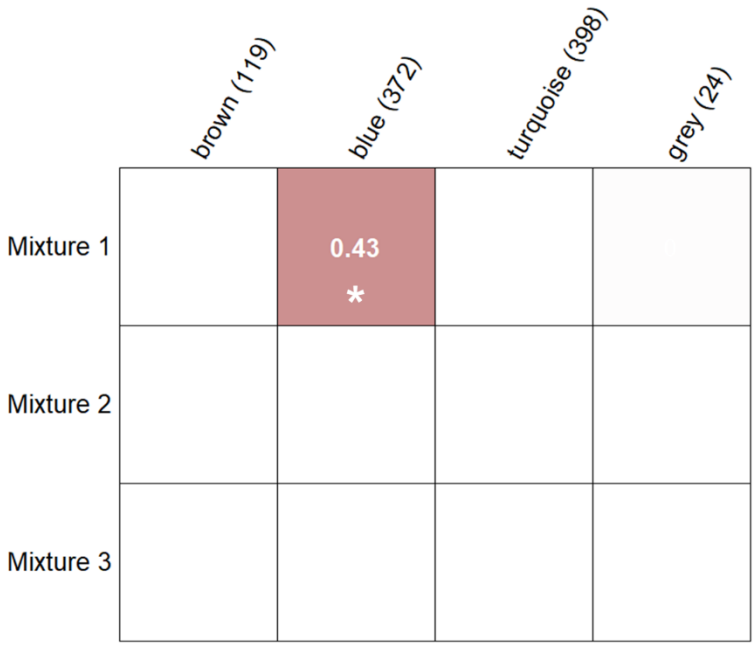

Figure 6. Correlations between module eigengenes (columns) and trace element mixtures (rows) for the red muscle proteome. Values in brackets with module names indicate the number of proteins belonging to each module. Values in the cells are Spearman's correlation coefficients. Blank cells indicate non-significant correlation (P>0.05). *: P<0.05, **: P<0.01

Only the blue module correlated (positively) with one contaminant mixture (i.e., mixture 1, Figure 6). This module was enriched in cellular organization and ion transport pathways (Figure 7 and ESM8). According to the cellular component enrichment analysis, proteins were mainly located in membranes (ESM8b).

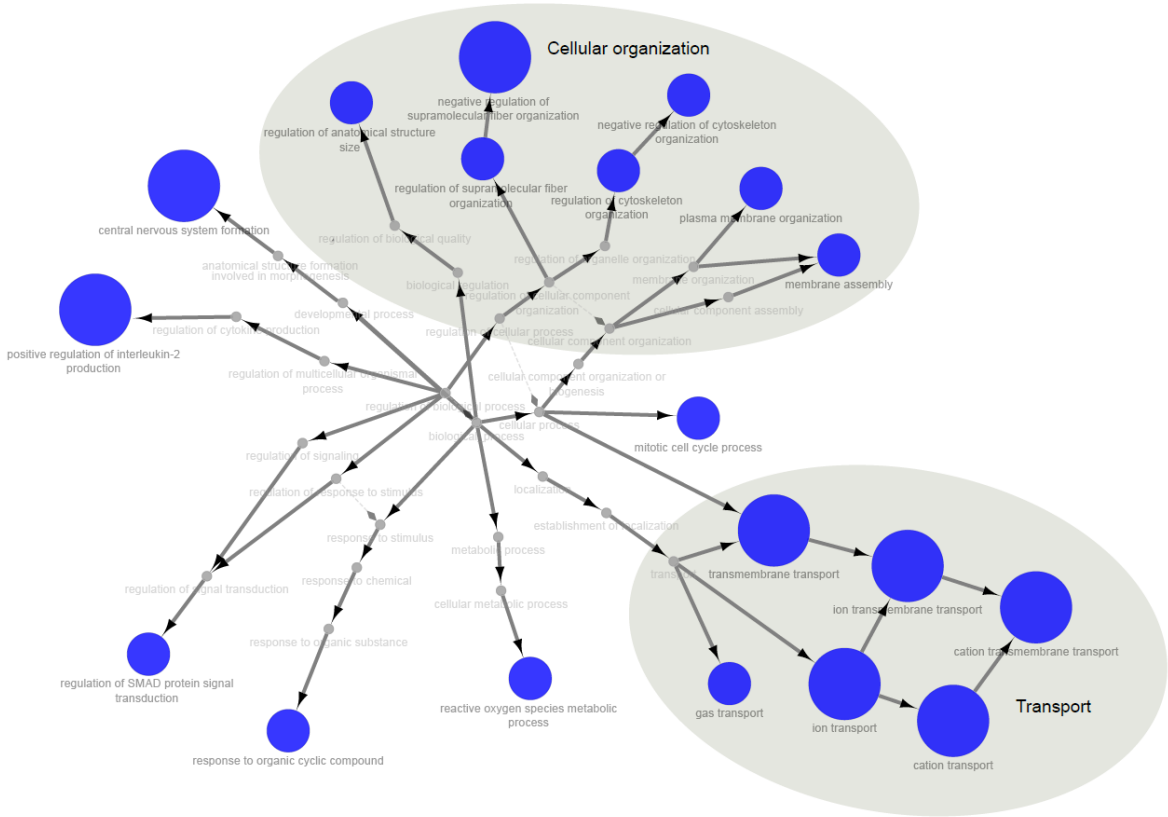

Figure 7. Significant GO terms (FDR <0.001) and ontological relationships in red muscle. Circle size indicates the level of FDR-adjusted statistical significance. Biological processes were grouped in larger pathways (large grey circles).

Two identified hubproteins for the blue module have a known function in the response to oxidative stress (Gluthatione S-transferase and Hemoglobin subunit zeta), whereas two others are involved in cellular structure and muscle contraction (myosin-binding protein H and Myomesin-2). The last identified hubprotein was the ADP/ATP translocase 1 which is implicated in energy metabolism and apoptosic signaling pathway (Table 3).

Table 3. Top 5 hubproteins selected for each co-expression module in the red muscle proteome. The name and UniprotKB ID are indicated for each of them as well as their main functions, their module, their expression pattern (up or down-regulation), contaminant mixture they correlate with and the module membership.

Name	UniprotKB ID	Module	Main function	Expression pattern	Principal Component	Module membership
Glutathione S-transferase	LANCL1	blue	Contaminant detoxification, Oxidative stress metabolism	↓ down	PC1	-0.92
Hemoglobin subunit zeta	HBZ	blue	Gas transport, Oxidative stress metabolism	↑ up	PC1	0.90
Myosin-binding protein H	MYBPH	blue	Cell adhesion, Muscle contraction	↓ down	PC1	-0.92
ADP/ATP translocase 1	SLC25A4	blue	Transmembrane transporter, Apoptosic signalling pathway	↓ down	PC1	-0.92
Myomesin-2	MYOM2	blue	Cellular organization, Muscle contraction	↓ down	PC1	-0.91

Comparison of liver vs red muscle proteome response

Comparison of the delta-rank values obtained from GO enrichment analysis for both tissues against mixture 1 revealed a significant positive correlation (r = 0.22, P<0.001 ESM9a). Liver and muscle enrichment for mixture 2 displayed no significant correlation (r = 0.02, P = 0.96, ESM9b), while enrichment for mixture 3 revealed a significant but weak positive correlation between the two tissues (r =

0.06, P<0.01, ESM9c). This highlights that similar processes appear involved in liver and red muscle in response to contaminant mixture 1 and, to a lesser extent, mixture 3.

Discussion

Multiple studies have investigated the potential drivers of the drastic decrease in size, age and body condition of sardines in the Gulf of Lions since 2008 (e.g. Brosset et al., 2015, 2016, 2017; Le Bourg et al., 2015; Van Beveren et al., 2016, 2017; Feuilloley et al. 2020). However, thorough information on chemical contamination by trace elements and its physiological impact on this species was lacking. We found evidence for the accumulation of multiple elements in sardines, with a light East-West contamination gradient within the Gulf of Lions. While macro-physiological parameters (i.e. body condition) were not affected by contamination, pathways involved in cellular organization and response to stress were clearly upregulated, particularly in the liver, but also in muscle. In addition, a global upregulation in processes linked to the immune system and lipid homeostasis was recorded in the liver. We are proposing biomarkers of the effects of trace element stress on health, which could serve as a starting point in biomonitoring programs.

Contamination load in the Mediterranean sardine of the Gulf of Lions

The impact of contaminating loads from the Rhône River on the organisms living in the Gulf of Lions has already been reported with regard to radionuclides, such as ^{210}Po (Strady et al. 2015), heavy metals (Cd, Pb and Hg for [60–200 µm] size fraction, Chouvelon et al., 2019) and organic contaminants, such as Polychlorinated biphenyls (PCBs) in plankton (Alekseenko et al. 2018). In addition to the Rhône River inputs, pollutant discharges are also likely to come from industrial and urban activities of the nearby cities of Marseille and Fos-sur-Mer. Small pelagic planktivorous fish such as sardines in the eastern areas of the Gulf of Lions might therefore be highly exposed to chemical contamination, notably via trophic pathways (i.e. plankton). Interestingly, although large inter-individual variability in contamination between individuals was recorded in our study, we noted a moderate East to West contamination gradient in the Gulf of Lions. These results differ from previous work (Chouvelon et al. 2019) that did not detect a spatial pattern in trace element contamination in the same species and location. These differences might be due to the targeted tissue, as they considered contamination in the whole organism (liver, muscle, gonad and remaining tissues) whereas we focused on muscle contamination. Indeed, factors such as tissue-specific metabolic processes, affinity for contaminants and turnover rates can contribute to distinct contamination patterns observed across differents tissues. Another reason for discrepancies between our and previous studies might involve the fact that individuals were sampled at different life stages in those former studies, whereas we focused on individuals in their first year of life (age 0). Indeed, confounding effects with contaminant elimination through reproduction as well as bioaccumulation with age may explain large variations and no clear spatial pattern (Bodiguel et al. 2009). Canli and Atli (2003) highlighted the importance of fish size in determining the rate of physiological processes, as size may influence the uptake, distribution, and elimination of trace elements. In our study, only three trace elements (out of 13) displayed significant relationships with fish size, namely Pb, Rb and Tl. This lack of relationship with size for most of trace elements could result from the complexity of bioaccumulation processes involving interaction between various routes of absorption, excretion, passive release, and metabolization (Joiris et al. 1999; Guo et al. 2016; Tang et al. 2017). Yet, the study of one-year-old gilthead seabream juveniles (Beauvieux et al. 2024) showed comparable outcomes. This indicates that when examining a single age group, size differences are likely minimal, simplifying the study of spatial contamination. That said, exploring multiple age groups remains essential to uncover intricate bio-accumulation patterns.

Trace metal concentrations in Mediterranean surface waters and top predators are generally higher than in the Atlantic Ocean (Boyle et al. 1985; Cossa and Coquery 2005). It is suggested that it could be due to the enhanced ability of Mediterranean pelagic food chains to bioaccumulate certain chemicals, as documented for mercury (Cossa and Coquery 2005; Harmelin-Vivien et al. 2009; Chouvelon et al. 2018). This pattern also turned out to be true for As, Ni, Cr, Pb, Zn and Hg in sardines recorded in numerous studies (considering only *S. pilchardus* in ESM10). Trace element concentrations found in the present study were of a similar order of magnitude to those found in other studies focusing on the same or close

species of the Mediterranean, Atlantic or Indian Oceans, except for lithium. Averaged Li levels were 32 times higher than those found by Guérin et al. (2011) on the Mediterranean sardine (but Li levels were measured in only 4 individuals in this previous work) and 2 times higher than those found by Lozano-Bilbao et al. (2019) on *S. pilchardus* in the Atlantic Ocean.

Similarly to findings in seabreams (Beauvieux et al. 2024), we identified a lack of monitoring for several elements including Li, Rb, Sr, Ti and Tl in all locations (Indian and Atlantic Oceans and the Mediterranean Sea, ESM10 and ESM11). This is partially explained by the absence of regulatory limits for these elements in fish muscle (along with Cr and Ni), despite their increasing use in multiple areas (industrial, agriculture, high-tech and medication industries) and despite their toxicity for organisms (Exley et al. 1991; Authman 2011; Aslam and Yousafzai 2017; Blewett and Leonard 2017; Kumari et al. 2017; Genchi et al. 2021).

The European regulation sets contamination thresholds for only three specific inorganic trace elements, Pb (lead), Cd (cadmium) and Hg (mercury). In contrast, other nations, such as Turkey and Greece have adopted thresholds for a larger set of contaminants (for a comprehensive review, refer to Guerra-García et al., 2023). Notably, trace element levels in sardine specimens from the present study remained below the threshold values for fish consumption set by most international regulations except for As that exceeded these limits. These findings emphasize the need for further efforts by the European commission and other institutions to establish health limits not only for Arsenic but also for other nonessential and essential elements.

Commonly dysregulated pathways in the liver and red muscle in response to multiple-metal contamination

Liver and red muscle shared common proteome changes, such as cellular disorganisation as well as functions involved in transport and stress response (Figure 5 and 7). This is in line with the positive correlation found between the functional enrichment of the two tissues in relation to mixture 1 and mixture 3 (ESM9), highlighting similar responses (up-regulation). However, we noted a much more intense response in the liver, with 17 times more pathways overexpressed compared to red muscle. Similar results have been observed in seabreams (Beauvieux et al. 2024). This discrepancy in responses between both tissues could be related to the liver functions, as this is the main organ responsible for detoxification, transformation and storage of toxic compounds in fish (Bawuro et al. 2018; Beauvieux et al. 2024).

Contaminant mixture 1 (contamination in Cu, Rb, Sr, Tl, Zn, Li, Pb and As) seemed to particularly impact cellular organization in the two tissues, as reflected by an overexpression of multiple pathways involved in cellular structure, intracellular transport and motility processes. In particular, two isoforms of cytoplasmic dynein heavy chain seemed to be affected by mixture 1 in liver (along with mixture 3). Cytoplasmic dyneins are central in intracellular trafficking, including macromolecular transport, chromosome dynamics, and the cell cycle (Paschal et al. 1987; Kardon and Vale 2009; Bawuro et al. 2018). This is in line with the significant downregulation in the pathway involved in mitotic spindle assembly that has been also detected and could indicate that trace-element exposure has genotoxic effects and may repress hepatocyte division. Similarly, cytoplasmic dyneins (Table 2) were identified in bivalves as responsive to contamination (Li & Wang, 2021; Sánchez-Marín et al., 2021), which made them great candidate biomarkers of trace element contamination. Additionally, given that proper cellular organization is crucial for organismal development, the abundance of upregulated pathways associated with anatomical structure and development may suggest a response to counteract contamination-induced disorganization. Histopathological alterations in hepatocytes have already been observed, revealing the disorganization of organelles within the cytoplasm (Moreira et al. 2003) and the presence of necrosis (Javed et al. 2017) in response to metal contamination. Since hepatocytes are involved in various aspects of intermediate metabolism, unfavourable consequences to physiology may be expected as well at the cellular and organismal level (Mela et al. 2007).

Red muscle proteome response to mixture 1 was less marked than that of the liver proteome, but it reflected an alteration of the biological structure of cells and, again, the cell cycle process, as highlighted by the upregulation of the pathway “mitotic cell cycle process”. Accordingly, two of the five hubproteins identified were myosin and myomesin, which are key proteins in cell adhesion and muscle contraction. This is consistent with previous works, that highlighted alterations of multiple myocytoskeleton proteins

in response to contamination (Rodríguez-Ortega et al. 2003; Karim et al. 2011; Xu et al. 2019). As the contractile ability of myocytes resides in their highly organized cytoskeleton network, dysregulation here could greatly affect the locomotion of juvenile sardines, hindering their escape from predators and their foraging success.

The effects of trace element contamination on liver and muscle cytoskeleton are likely to be caused by oxidative stress (Epel et al. 2004), either through excess reactive oxygen species (ROS) generation (by redox-active metals) or reduction of antioxidant abundances and or activities (redox-inactive metals) (Koivula and Eeva 2010). In this study, we highlighted the upregulation of pathways such as "cellular oxidant detoxification" and "hydrogen peroxide catabolic process" in the liver and "reactive oxygen species metabolic process" in muscle. Consequently, two potential biomarkers of red muscle proteome in response to mixture 1 were identified (down-regulated gluthathione S-transferase and up-regulated hemoglobin subunit zeta, Table 3). They have both known functions in contaminant detoxification and antioxidant defences, respectively (Mollan et al. 2012). Gluthathione S-transferase was underexpressed in red muscle with increasing contamination (mixture 1), suggesting a redox-inactive potential of mixture 1 on this enzyme specifically but also highlighting that some canonical detoxification enzymes may be triggered or repressed by metal exposure, depending on their intrinsic nature (redox-active *vs* redox-inactive sensitivity).

Furthermore, trace element mixtures induced additional cellular responses aimed at safeguarding organisms from ROS-induced damage. Among these responses, a heat shock protein homologue (Dnaj homologue, Table 2) plays a crucial role by acting as cochaperones to the molecular chaperone (Hsp70). Its functions involve protein translation, promoting protein folding, translocation of polypeptides through membranes and degradation of damaged proteins (Mitra et al. 2009). In multicellular eukaryotes, programmed cell death, often referred to as apoptosis, is a prevalent stress response mechanism that comes into play when the level of stress surpasses the cell's ability to uphold genomic and macromolecular integrity. In this study, apoptosis signalling pathway involving ADP/ATP translocase and the serine/threonine-protein kinase mTOR (Table 3 and Table 2) appeared to be affected by trace element contamination. Previous transcriptomics and proteomics studies have reported alterations in apoptotic pathways in various fish species in response to environmental contaminants (Bohne-Kjersem et al. 2009; Leaver et al. 2010; Asker et al. 2013; Yadetie et al. 2013). The serine/threonine-protein kinase mTOR was overexpressed in response to trace element contamination in the liver, which is implicated in cellular death cascades along with lipid regulation and nutrient signaling. The activation of the signalling network mTOR has been associated with organic and inorganic contaminants-induced apoptosis (Chen et al. 2008; McCuaig et al. 2020). Moreover, the ADP/ATP translocase is suggested to play a significant role in the process of mitochondrial permeabilization as it can switch its function from ADP/ATP exchange through inner mitochondrial membrane to pore-formation during apoptosis (Kumarswamy and Chandna 2009). Therefore, these two proteins could be excellent candidates biomarker for trace element effects in liver in red muscle.

Metabolism and immune system up-regulation in liver

Trace element contamination (mixtures 1 and 3) appeared to specifically affect the metabolism and transport of lipids in the liver, as reflected by the overexpression of two apolipoproteins (hubproteins). Lipids are an energy source and an essential component of cell membranes (phospholipids and cholesterol). Besides, they also play a significant role as messengers in signal transduction pathways and molecular recognition processes (Van Meer et al. 2008). Any changes in lipid metabolism would signal impairment of these pathways. It has been reported that constant energy demand leads to mobilization of triglycerides as they serve as lipid storage (Van Meer et al. 2008; Santos and Schulze 2012). The upregulation of triglyceride metabolic process and transport underlined in this study could be an evidence of their mobilization and use in repair or development of membranes damaged, for instance under increasing oxidative stress (Van Meer et al. 2008; Santos and Schulze 2012)(Santos and Schulze 2012). Their mobilization and transport may also be linked to low food intake or absorption due to gut damage or improper synthesis in the liver under trace element stress. In the absence of further research to shed light on these regulation patterns, we propose here two promising biomarkers that may indicate a dysregulation in lipid transport and metabolism in response to contamination: apolipoprotein B-100 and apolipoprotein A-IV (see Table 2) that were found upregulated in our study but also in seahorses and

atlantic cod in response to heavy metal and organic contaminant stress respectively (Bohne-Kjersem et al. 2009; Liu et al. 2022). These proteins are important regulators of triglyceride and cholesterol metabolism (Sacks 2006). By studying these potential biomarkers, we can gain valuable insights into the effects of metal contamination on lipid-related processes.

The sardine liver proteome also presented a clear up-regulation in multiple pathways involved in immune processes. Regoli & Giuliani (2014) and Wang & Gallagher (2013) highlighted that such an up-regulation could be related to trace element accumulation in the liver and lead to increasing oxidative stress. The fish immune system is known to be sensitive to environmental contamination (Si et al. 2019) and altering immune homeostasis in fish could significantly constrain their survival and development. Sustaining high levels of immune functions requires energy, which would be necessarily redirected from other mains functions, such as growth, reproduction or maintenance (energy trade-off, ; Moret & Schmid-Hempel, 2000).

In our experiment we did not find any correlation between body condition and contamination mixtures. This is consistent with some other studies that investigated the relationship between metal levels in the environment or fish tissues and body condition (Farag et al. 1998; Dethloff et al. 2001; Lohner et al. 2001). The measurement of body mass may not sufficiently illustrate the costs of metal exposure, since individuals can balance their resource budget and adjust their body condition over a longer period (Daan et al. 1996, Beauvieux et al. 2022). The absence of relationship could also suggest that body condition, although a great marker of nutritional stress (Brosset et al., 2015), only declines drastically when a high threshold of physiological stress is reached. Therefore, monitoring physiological processes that are more sensitive and reflect progressive changes might allow to detect early warnings of environmental challenges. Nonetheless, sardines from the Mediterranean Sea have shown a drastic decline in body condition, size and life expectancy in the past two decades (Saraux et al. 2019). The major driver proposed is the shift of sardine diet towards smaller planktonic prey observed in the Gulf of Lions due to multi-factorial environmental changes (Feuillolley et al 2020, Brosset et al., 2016), leading to lower foraging efficiency and a reallocation trade-off toward reproduction instead of survival (Brosset et al. 2016b; Queiros 2019; Beauvieux et al. 2022). Consequently, individuals at the end of the reproduction period may rely on low energetic reserves to survive the end of the winter period. Adding any additional energetic or immune burden, as those highlighted in response to contaminants in this study, might emphasize their reduced chance of survival (Queiros et al. 2021).

Acknowledgements

We are grateful to the technical and scientific crews of L'Europe for their work during PELMED survey.

Data, scripts, code, and supplementary information availability

The mass spectrometry proteomics data have been deposited to the ProteomeXchange Consortium via the PRIDE (Perez-Riverol et al. 2019) partner repository with the dataset identifiers PXD037276 (liver) and PXD037313 (red muscle).

Conflict of interest disclosure

The authors declare that they comply with the PCI rule of having no financial conflicts of interest in relation to the content of the article.

Funding

This work is part of the project ICIPOP granted by the "Agence Francaise de Developpement" (AFD). A. B. has a PhD grant from University of Montpellier – GAIA doctoral school.

References

Alekseenko E, Thouvenin B, Tronczyński J, Carlotti F, Garreau P, Tixier C, Baklouti M (2018) Modeling of PCB trophic transfer in the Gulf of Lions; 3D coupled model application. Mar Pollut Bull 128:140–155

Apraiz I, Mi J, Cristobal S (2006) Identification of proteomic signatures of exposure to marine pollutants in mussels (Mytilus edulis). Mol Cell Proteomics 5:1274–1285

Asaduzzaman K, Khandaker MU, Binti Baharudin NA, Amin YBM, Farook MS, Bradley DA, Mahmoud O (2017) Heavy metals in human teeth dentine: A bio-indicator of metals exposure and environmental pollution. Chemosphere 176:221–230

Asker N, Kristiansson E, Albertsson E, Larsson DGJ, Förlin L (2013) Hepatic transcriptome profiling indicates differential mRNA expression of apoptosis and immune related genes in eelpout (Zoarces viviparus) caught at Göteborg harbor, Sweden. Aquat Toxicol 130–131:58–67

Aslam S, Yousafzai AM (2017) Chromium toxicity in fish: A review article. ~ 1483 ~ J Entomol Zool Stud 5:1483–1488

Authman MMN (2011) Environmental and experimental studies of aluminium toxicity on the liver of oreochromis niloticus (Linnaeus, 1757) fish. Life Sci J 8:764–776

Baker E, Sevaldsen P, Kurvits T (2013) State and pressures of the marine and coastal Mediterranean environment.

Bawuro AA, Voegborlo RB, Adimado AA (2018) Bioaccumulation of Heavy Metals in Some Tissues of Fish in Lake Geriyo, Adamawa State, Nigeria. J Environ Public Health 2018:

Beauvieux A, Fromentin J-M, Romero D, Couffin N, Brown A, Metral L, Bourjea J, Bertile F, Schull Q (2024) Molecular fingerprint of gilthead seabream physiology in response to pollutant mixtures in the wild. Environ Pollut 340:122789

Beauvieux A, Queiros Q, Metral L, Dutto G, Gasset E, Criscuolo F, Fromentin JM, Saraux C, Schull Q (2022) Energy allocation trade-offs between life-history traits in the Mediterranean sardine: an ecophysiological approach. Mar Ecol Prog Ser 701:99–118

Benninghoff AD (2007) Toxicoproteomics - The next step in the evolution of environmental biomarkers? Toxicol Sci 95:1–4

Bervoets L, Blust R (2003) Metal concentrations in water, sediment and gudgeon (Gobio gobio) from a pollution gradient: Relationship with fish condition factor. Environ Pollut 126:9–19

Bervoets L, Knaepkens G, Eens M, Blust R (2005) Fish community responses to metal pollution. Environ Pollut 138:338–349

Van Beveren E, Fromentin J-M, Rouyer T, Bonhommeau S, Brosset P, Saraux C (2016a) The fisheries history of small pelagics in the Northern Mediterranean. ICES J Mar Sci 73:1475–1484

Van Beveren E, Fromentin JM, Bonhommeau S, Nieblas AE, Metral L, Brisset B, Jusup M, Bauer RK, Brosset P, Saraux C (2017) Predator–prey interactions in the face of management regulations: Changes in Mediterranean small pelagic species are not due to increased tuna predation. Can J Fish Aquat Sci 74:1422–1430

Van Beveren E, Keck N, Fromentin JM, Laurence S, Boulet H, Labrut S, Baud M, Bigarré L, Brosset P, Saraux C (2016b) Can pathogens alter the population dynamics of sardine in the NW Mediterranean? Mar Biol 163:240

Bindea G, Mlecnik B, Hackl H, Charoentong P, Tosolini M, Kirilovsky A, Fridman W-H, Pagès F, Trajanoski Z,

Galon J (2009) ClueGO: a Cytoscape plug-in to decipher functionally grouped gene ontology and pathway annotation networks. Bioinformatics 25:1091–1093

Blewett TA, Leonard EM (2017) Mechanisms of nickel toxicity to fish and invertebrates in marine and estuarine waters. Environ Pollut 223:311–322

Bodiguel X, Loizeau V, Le Guellec AM, Roupsard F, Philippon X, Mellon-Duval C (2009) Influence of sex, maturity and reproduction on PCB and p,p'DDE concentrations and repartitions in the European hake (Merluccius merluccius, L.) from the Gulf of Lions (N.W. Mediterranean). Sci Total Environ 408:304–311

Bohne-Kjersem A, Skadsheim A, Goksøyr A, Grøsvik BE (2009) Candidate biomarker discovery in plasma of juvenile cod (Gadus morhua) exposed to crude North Sea oil, alkyl phenols and polycyclic aromatic hydrocarbons (PAHs). Mar Environ Res 68:268–277

Bourdeix J, Hattab T (1985) PELMED - PELAGIQUES MEDITERRANÉE.

Le Bourg B, Bănaru D, Saraux C, Nowaczyk A, Le Luherne E, Jadaud A, Bigot JL, Richard P (2015) Trophic niche overlap of sprat and commercial small pelagic teleosts in the Gulf of Lions (NW Mediterranean Sea). J Sea Res 103:138–146

Boyle EA, Chapnick SD, Bai XX, Spivack A (1985) Trace metal enrichments in the Mediterranean Sea. Earth Planet Sci Lett 74:405–419

Braasch I, Gehrke AR, Smith JJ, Kawasaki K, Manousaki T, Pasquier J, Amores A, Desvignes T, Batzel P, Catchen J, Berlin AM, Campbell MS, Barrell D, Martin KJ, Mulley JF, Ravi V, Lee AP, Nakamura T, Chalopin D, Fan S, Wcisel D, Cañestro C, Sydes J, Beaudry FEG, Sun Y, Hertel J, Beam MJ, Fasold M, Ishiyama M, Johnson J, Kehr S, Lara M, Letaw JH, Litman GW, Litman RT, Mikami M, Ota T, Saha NR, Williams L, Stadler PF, Wang H, Taylor JS, Fontenot Q, Ferrara A, Searle SMJ, Aken B, Yandell M, Schneider I, Yoder JA, Volff J-N, Meyer A, Amemiya CT, Venkatesh B, Holland PWH, Guiguen Y, Bobe J, Shubin NH, Di Palma F, Alföldi J, Lindblad-Toh K, Postlethwait JH (2016) The spotted gar genome illuminates vertebrate evolution and facilitates human-teleost comparisons. Nat Genet 48:427–437

Broche P, Devenon JL, Forget P, De Maistre JC, Naudin JJ, Cauwet G (1998) Experimental study of the Rhone plume. Part I: Physics and dynamics. Oceanol Acta 21:725–738

Brosset P, Le Bourg B, Costalago D, BĂnaru D, Van Beveren E, Bourdeix JH, Fromentin JM, Ménard F, Saraux C (2016a) Linking small pelagic dietary shifts with ecosystem changes in the Gulf of Lions. Mar Ecol Prog Ser 554:157–171

Brosset P, Fromentin JM, Van Beveren E, Lloret J, Marques V, Basilone G, Bonanno A, Carpi P, Donato F, Čikeš Keč V, De Felice A, Ferreri R, Gašparević D, Giráldez A, Gücü A, Iglesias M, Leonori I, Palomera I, Somarakis S, Tičina V, Torres P, Ventero A, Zorica B, Ménard F, Saraux C (2017) Spatio-temporal patterns and environmental controls of small pelagic fish body condition from contrasted Mediterranean areas. Prog Oceanogr 151:149–162

Brosset P, Fromentin JM, Ménard F, Pernet F, Bourdeix JH, Bigot JL, Van Beveren E, Pérez Roda MA, Choy S, Saraux C (2015a) Measurement and analysis of small pelagic fish condition: A suitable method for rapid evaluation in the field. J Exp Mar Bio Ecol 462:90–97

Brosset P, Lloret J, Muñoz M, Fauvel C, Van Beveren E, Marques V, Fromentin JM, Ménard F, Saraux C (2016b) Body reserves mediate trade-offs between life-history traits: New insights from small pelagic fish reproduction. R Soc Open Sci 3:

Brosset P, Ménard F, Fromentin JM, Bonhommeau S, Ulses C, Bourdeix JH, Bigot JL, Van Beveren E, Roos D, Saraux C (2015b) Influence of environmental variability and age on the body condition of small pelagic fish in the Gulf of Lions. Mar Ecol Prog Ser 529:219–231

Bucchia M, Camacho M, Santos MRD, Boada LD, Roncada P, Mateo R, Ortiz-Santaliestra ME, Rodríguez-Estival

J, Zumbado M, Orós J, Henríquez-Hernández LA, García-Álvarez N, Luzardo OP (2015) Plasma levels of pollutants are much higher in loggerhead turtle populations from the Adriatic Sea than in those from open waters (Eastern Atlantic Ocean). Sci Total Environ 523:161–169

Carapito C, Burel A, Guterl P, Walter A, Varrier F, Bertile F, Van Dorsselaer A (2014) MSDA, a proteomics software suite for in-depth Mass Spectrometry Data Analysis using grid computing. Proteomics 14:1014–1019

Celander MC (2011) Cocktail effects on biomarker responses in fish. Aquat Toxicol 105:72–77

Chen L, Liu L, Luo Y, Huang S (2008) MAPK and mTOR pathways are involved in cadmium-induced neuronal apoptosis. J Neurochem 105:251–261

Chouvelon T, Cresson P, Bouchoucha M, Brach-Papa C, Bustamante P, Crochet S, Marco-Miralles F, Thomas B, Knoery J (2018) Oligotrophy as a major driver of mercury bioaccumulation in medium-to high-trophic level consumers: A marine ecosystem-comparative study. Environ Pollut 233:844–854

Chouvelon T, Strady E, Harmelin-Vivien M, Radakovitch O, Brach-Papa C, Crochet S, Knoery J, Rozuel E, Thomas B, Tronczynski J, Chiffoleau J-F (2019) Patterns of trace metal bioaccumulation and trophic transfer in a phytoplankton-zooplankton-small pelagic fish marine food web. Mar Pollut Bull 146:1013–1030

Cossa D, Coquery M (2005) The Mediterranean Mercury Anomaly, a Geochemical or a Biologocal Issue. pp 177–208

Cossa D, Durrieu de Madron X, Schäfer J, Lanceleur L, Guédron S, Buscail R, Thomas B, Castelle S, Naudin JJ (2017) The open sea as the main source of methylmercury in the water column of the Gulf of Lions (Northwestern Mediterranean margin). Geochim Cosmochim Acta 199:222–237

Denslow ND, Knoebl I, Larkin P (2005) Chapter 3 Approaches in proteomics and genomics for eco-toxicology. Biochem Mol Biol Fishes 6:85–116

Dethloff GM, Bailey HC, Maier KJ (2001) Effects of dissolved copper on select hematological, biochemical, and immunological parameters of wild rainbow trout (Oncorhynchus mykiss). Arch Environ Contam Toxicol 40:371–380

Dixon GB, Davies SW, Aglyamova GA, Meyer E, Bay LK, Matz M V. (2015) Genomic determinants of coral heat tolerance across latitudes. Science (80-) 348:1460–1462

Downs CA, Richmond RH, Mendiola WJ, Rougée L, Ostrander GK (2006) Cellular physiological effects of the MV Kyowa Violet fuel-oil spill on the hard coral, Porites lobata. Environ Toxicol Chem 25:3171–3180

Durrieu de Madron X, Guieu C, Sempéré R, Conan P, Cossa D, D'Ortenzio F, Estournel C, Gazeau F, Rabouille C, Stemmann L, Bonnet S, Diaz F, Koubbi P, Radakovitch O, Babin M, Baklouti M, Bancon-Montigny C, Belviso S, Bensoussan N, Bonsang B, Bouloubassi I, Brunet C, Cadiou J-F, Carlotti F, Chami M, Charmasson S, Charrière B, Dachs J, Doxaran D, Dutay J-C, Elbaz-Poulichet F, Eléaume M, Eyrolles F, Fernandez C, Fowler S, Francour P, Gaertner JC, Galzin R, Gasparini S, Ghiglione J-F, Gonzalez J-L, Goyet C, Guidi L, Guizien K, Heimbürger L-E, Jacquet SHM, Jeffrey WH, Joux F, Le Hir P, Leblanc K, Lefèvre D, Lejeusne C, Lemé R, Loÿe-Pilot M-D, Mallet M, Méjanelle L, Mélin F, Mellon C, Mérigot B, Merle P-L, Migon C, Miller WL, Mortier L, Mostajir B, Mousseau L, Moutin T, Para J, Pérez T, Petrenko A, Poggiale J-C, Prieur L, Pujo-Pay M, Pulido-Villena, Raimbault P, Rees AP, Ridame C, Rontani J-F, Ruiz Pino D, Sicre MA, Taillandier V, Tamburini C, Tanaka T, Taupier-Letage I, Tedetti M, Testor P, Thébault H, Thouvenin B, Touratier F, Tronczynski J, Ulses C, Van Wambeke F, Vantrepotte V, Vaz S, Verney R (2011) Marine ecosystems' responses to climatic and anthropogenic forcings in the Mediterranean. Prog Oceanogr 91:97–166

Dydak U, Jiang YM, Long LL, Zhu H, Chen J, Li WM, Edden RAE, Hu S, Fu X, Long Z, Mo XA, Meier D, Harezlak J, Aschner M, Murdoch JB, Zheng W (2011) In vivo measurement of brain GABA concentrations by magnetic resonance spectroscopy in smelters occupationally exposed to manganese. Environ Health Perspect 119:219–224

Epel ES, Blackburn EH, Lin J, Dhabhar FS, Adler NE, Morrow JD, Cawthon RM (2004) Accelerated telomere shortening in response to life stress. Proc Natl Acad Sci U S A 101:17312–17315

Exley C, Chappell JS, Birchall JD (1991) A mechanism for acute aluminium toxicity in fish. J Theor Biol 151:417–428

Farag AM, Woodward DF, Goldstein JN, Brumbaugh W, Meyer JS (1998) Concentrations of metals associated with mining waste in sediments, biofilm, benthic macroinvertebrates, and fish from the Coeur d'Alene River Basin, Idaho. Arch Environ Contam Toxicol 34:119–127

Folch J, Lees M, Stanley GHS (1957) A simple method for the isolation and purification of total lipides from animal tissues. J Biol Chem 226:497–509

Genchi G, Carocci A, Lauria G, Sinicropi MS, Catalano A (2021) Thallium Use, Toxicity, and Detoxification Therapy: An Overview. Appl Sci 11:8322

Guérin T, Chekri R, Vastel C, Sirot V, Volatier JL, Leblanc JC, Noël L (2011) Determination of 20 trace elements in fish and other seafood from the French market. Food Chem 127:934–942

Guerra-García JM, Calero-Cano S, Donázar-Aramendía Í, Giráldez I, Morales E, Arechavala-Lopez P, Cervera-Currado JL (2023) Assessment of elemental composition in commercial fish of the Bay of Cádiz, Southern Iberian Peninsula. Mar Pollut Bull 187:

Guo Z, Zhang W, Du S, Green I, Tan Q, Zhang L (2016) Developmental patterns of copper bioaccumulation in a marine fish model Oryzias melastigma. Aquat Toxicol 170:216–222

Halliwell B, Gutteridge JMC (2015) Free Radicals in Biology and Medicine. Oxford University Press,

Harmelin-Vivien M, Cossa D, Crochet S, Bănaru D, Letourneur Y, Mellon-Duval C (2009) Difference of mercury bioaccumulation in red mullets from the north-western Mediterranean and Black seas. Mar Pollut Bull 58:679–685

Heys KA, Shore RF, Pereira MG, Jones KC, Martin FL (2016) Risk assessment of environmental mixture effects. RSC Adv 6:47844–47857

Hollis L, McGeer JC, McDonald DG, Wood CM (1999) Cadmium accumulation, gill Cd binding, acclimation, and physiological effects during long term sublethal Cd exposure in rainbow trout. Aquat Toxicol 46:101–119

Isani G, Andreani G, Cocchioni F, Fedeli D, Carpené E, Falcioni G (2009) Cadmium accumulation and biochemical responses in Sparus aurata following sub-lethal Cd exposure. Ecotoxicol Environ Saf 72:224–230

Javed M, Ahmad MI, Usmani N, Ahmad M (2017) Multiple biomarker responses (serum biochemistry, oxidative stress, genotoxicity and histopathology) in Channa punctatus exposed to heavy metal loaded waste water. Sci Rep 7:1675

Joiris CR, Holsbeek L, Moatemri NL (1999) Total and methylmercury in sardines Sardinella aurita and Sardina pilchardus from Tunisia. Mar Pollut Bull 38:188–192

Kardon JR, Vale RD (2009) Regulators of the cytoplasmic dynein motor. Nat Rev Mol Cell Biol 10:854–865

Karim M, Puiseux-Dao S, Edery M (2011) Toxins and stress in fish: Proteomic analyses and response network. Toxicon 57:959–969

Kaushal SS, Gold AJ, Bernal S, Johnson TAN, Addy K, Burgin A, Burns DA, Coble AA, Hood E, Lu YH, Mayer P, Minor EC, Schroth AW, Vidon P, Wilson H, Xenopoulos MA, Doody T, Galella JG, Goodling P, Haviland K, Haq S, Wessel B, Wood KL, Jaworski N, Belt KT (2018) Watershed 'chemical cocktails': forming novel elemental combinations in Anthropocene fresh waters. Biogeochemistry 141:281–305

Koivula MJ, Eeva T (2010) Metal-related oxidative stress in birds. Environ Pollut 158:2359–2370

Kumari B, Kumar V, Sinha AK, Ahsan J, Ghosh AK, Wang H, DeBoeck G (2017) Toxicology of arsenic in fish and aquatic systems. Environ Chem Lett 15:43–64

Kumarswamy R, Chandna S (2009) Putative partners in Bax mediated cytochrome-c release: ANT, CypD, VDAC or none of them? Mitochondrion 9:1–8

Langfelder P, Horvath S (2008) WGCNA: An R package for weighted correlation network analysis. BMC Bioinformatics 9:

Leaver MJ, Diab A, Boukouvala E, Williams TD, Chipman JK, Moffat CF, Robinson CD, George SG (2010) Hepatic gene expression in flounder chronically exposed to multiply polluted estuarine sediment: Absence of classical exposure “biomarker” signals and induction of inflammatory, innate immune and apoptotic pathways. Aquat Toxicol 96:234–245

Li Y, Wang WX (2021) Integrated transcriptomics and proteomics revealed the distinct toxicological effects of multi-metal contamination on oysters. Environ Pollut 284:117533

Liu Y, Shang D, Yang Y, Cui P, Sun J (2022) Transcriptomic Analysis Provides Insights into Microplastic and Heavy Metal Challenges in the Line Seahorse (Hippocampus erectus). Fishes 7:338

Lloret J, Shulman G, Love RM (2013) Condition and Health Indicators of Exploited Marine Fishes. John Wiley & Sons, Oxford

Lohner TW, Reash RJ, Willet VE, Rose LA (2001) Assessment of tolerant sunfish populations (Lepomis sp.) inhabiting selenium-laden coal ash effluents: 1. Hematological and population level assessment. Ecotoxicol Environ Saf 50:203–216

López-Pedrouso M, Varela Z, Franco D, Fernández JA, Aboal JR (2020) Can proteomics contribute to biomonitoring of aquatic pollution? A critical review. Environ Pollut 267:115473

Lozano-Bilbao E, Díaz Y, Lozano G, Jurado-Ruzafa A, Hardisson A, Rubio C, Jiménez S, González-Weller D, Gutiérrez ÁJ (2019) Metal Content in Small Pelagic Fish in the North-West Africa. Thalassas 35:643–653

McCuaig LM, Martyniuk CJ, Marlatt VL (2020) Morphometric and proteomic responses of early-life stage rainbow trout (Oncorhynchus mykiss) to the aquatic herbicide diquat dibromide. Aquat Toxicol 222:105446

Van Meer G, Voelker DR, Feigenson GW (2008) Membrane lipids: Where they are and how they behave. Nat Rev Mol Cell Biol 9:112–124

Mela M, Randi MAF, Ventura DF, Carvalho CEV, Pelletier E, Oliveira Ribeiro CA (2007) Effects of dietary methylmercury on liver and kidney histology in the neotropical fish Hoplias malabaricus. Ecotoxicol Environ Saf 68:426–435

Mitra A, Shevde LA, Samant RS (2009) Multi-faceted role of HSP40 in cancer. Clin Exp Metastasis 26:559–567

Mollan TL, Khandros E, Weiss MJ, Olson JS (2012) Kinetics of α-globin binding to α-Hemoglobin Stabilizing Protein (AHSP) indicate preferential stabilization of hemichrome folding intermediate. J Biol Chem 287:11338–11350

Morcillo P, Esteban M, Cuesta A (2016) Heavy metals produce toxicity, oxidative stress and apoptosis in the marine teleost fish SAF-1 cell line. Chemosphere 144:225–233

Moreira CM, Oliveira EM, Bonan CD, Sarkis JJF, Vassallo D V. (2003) Effects of mercury on myosin ATPase in the ventricular myocardium of the rat. Comp Biochem Physiol - C Toxicol Pharmacol 135:269–275

Moret Y, Schmid-Hempel P (2000) Survival for immunity: The price of immune system activation for bumblebee workers. Science (80-) 290:1166–1168

Parrish CC (1988) Dissolved and particulate marine lipid classes: a review. Mar Chem 23:17–40

Paschal BM, Shpetner HS, Vallee RB (1987) MAP 1C is a microtubule-activated ATPase which translocates microtubules in vitro and has dynein-like properties. J Cell Biol 105:1273–1282

Pedrotti ML, Petit S, Elineau A, Bruzaud S, Crebassa JC, Dumontet B, Martí E, Gorsky G, Cózar A (2016) Changes in the floating plastic pollution of the mediterranean sea in relation to the distance to land. PLoS One 11:1–14

Pereira S, Pinto AL, Cortes R, Fontaínhas-Fernandes A, Coimbra AM, Monteiro SM (2013) Gill histopathological and oxidative stress evaluation in native fish captured in Portuguese northwestern rivers. Ecotoxicol Environ Saf 90:157–166

Perez-Riverol Y, Csordas A, Bai J, Bernal-Llinares M, Hewapathirana S, Kundu DJ, Inuganti A, Griss J, Mayer G, Eisenacher M, Pérez E, Uszkoreit J, Pfeuffer J, Sachsenberg T, Yilmaz Ş, Tiwary S, Cox J, Audain E, Walzer M, Jarnuczak AF, Ternent T, Brazma A, Vizcaíno JA (2019) The PRIDE database and related tools and resources in 2019: Improving support for quantification data. Nucleic Acids Res 47:D442–D450

Plum LM, Rink L, Hajo H (2010) The essential toxin: Impact of zinc on human health. Int J Environ Res Public Health 7:1342–1365

Queiros Q (2019) Mechanisms underlying the bottom -up control of sardine populations in the Gulf of Lions : insight s from experiments and modeling. Université de Montpellier

Radakovitch O, Roussiez V, Ollivier P, Ludwig W, Grenz C, Probst JL (2008) Input of particulate heavy metals from rivers and associated sedimentary deposits on the Gulf of Lion continental shelf. Estuar Coast Shelf Sci 77:285–295

Regoli F, Giuliani ME (2014) Oxidative pathways of chemical toxicity and oxidative stress biomarkers in marine organisms. Mar Environ Res 93:106–117

Rodríguez-Ortega MJ, Grøsvik BE, Rodríguez-Ariza A, Goksøyr A, López-Barea J (2003) Changes in protein expression profiles in bivalve molluscs (Chamaelea gallina) exposed to four model environmental pollutants. Proteomics 3:1535–1543

Sacks FM (2006) The apolipoprotein story. Atheroscler Suppl 7:23–27

Sakuragui MM, Paulino MG, Pereira CDS, Carvalho CS, Sadauskas-Henrique H, Fernandes MN (2013) Integrated use of antioxidant enzymes and oxidative damage in two fish species to assess pollution in man-made hydroelectric reservoirs. Environ Pollut 178:41–51

Sanchez BC, Ralston-Hooper K, Sepúlveda MS (2011) Review of recent proteomic applications in aquatic toxicology. Environ Toxicol Chem 30:274–282

Santos CR, Schulze A (2012) Lipid metabolism in cancer. FEBS J 279:2610–2623

Saraux C, Van Beveren E, Brosset P, Queiros Q, Bourdeix J-H, Dutto G, Gasset E, Jac C, Bonhommeau S, Fromentin J-M (2019) Small pelagic fish dynamics: A review of mechanisms in the Gulf of Lions. Deep Sea Res Part II Top Stud Oceanogr 159:52–61

Sardenne F, Bodin N, Metral L, Crottier A, Le Grand F, Bideau A, Brisset B, Bourjea J, Saraux C, Bonhommeau S, Kerzérho V, Bernard S, Rouyer T (2019) Effects of extraction method and storage of dry tissue on marine lipids and fatty acids. Anal Chim Acta 1051:82–93

Si LF, Wang CC, Guo SN, Zheng JL, Xia H (2019) The lagged effects of environmentally relevant zinc on non-

specific immunity in zebrafish. Chemosphere 214:85–93

Souid G, Souayed N, Yaktiti F, Maaroufi K (2015) Lead accumulation pattern and molecular biomarkers of oxidative stress in seabream (Sparus aurata) under short-term metal treatment. Drug Chem Toxicol 38:98–105

Strady E, Harmelin-Vivien M, Chiffoleau JF, Veron A, Tronczynski J, Radakovitch O (2015) 210Po and 210Pb trophic transfer within the phytoplankton-zooplankton-anchovy/sardine food web: A case study from the Gulf of Lion (NW Mediterranean Sea). J Environ Radioact 143:141–151

Tang WL, Evans D, Kraemer L, Zhong H (2017) Body size-dependent Cd accumulation in the zebra mussel Dreissena polymorpha from different routes. Chemosphere 168:825–831

Teulier L, Thoral E, Queiros Q, McKenzie DJ, Roussel D, Dutto G, Gasset E, Bourjea J, Saraux C (2019) Muscle bioenergetics of two emblematic Mediterranean fish species: Sardina pilchardus and Sparus aurata. Comp Biochem Physiol -Part A Mol Integr Physiol 235:174–179

Tocher DR (2003) Metabolism and functions of lipids and fatty acids in teleost fish. Rev Fish Sci 11:107–184

Tournois J, Darnaude AM, Ferraton F, Aliaume C, Mercier L, McKenzie DJ (2017) Lagoon nurseries make a major contribution to adult populations of a highly prized coastal fish. Limnol Oceanogr 62:1219–1233

Tronczynski J, Carlotti F, Bodin N, Radakovitch O (2013) Contaminants bioaccumulation and biomagnification in a short trophic system: phytoplankton, zooplankton, anchovy, sardine (COSTAS). Ciesm

Wang L, Gallagher EP (2013) Role of Nrf2 antioxidant defense in mitigating cadmium-induced oxidative stress in the olfactory system of zebrafish. Toxicol Appl Pharmacol 266:177–186

Wang M, Wang Y, Zhang L, Wang J, Hong H, Wang D (2013) Quantitative proteomic analysis reveals the mode-of-action for chronic mercury hepatotoxicity to marine medaka (Oryzias melastigma). Aquat Toxicol 130–131:123–131

Williams CR, Yoshida-Honmachi EP (2013) Effects of cadmium on olfactory mediated behaviors and molecular biomarkers in coho salmon (Oncorhynchus kisutch). Aquat Toxicol 140–141:295–302

Wood C., Farell A., Brauner C. (2011) Copper of the Fish Physiology. Fish physiology. pp 55–133

Xu L, Lu Z, Ji C, Cong M, Li F, Shan X, Wu H (2019) Toxicological effects of As (V) in juvenile rockfish Sebastes schlegelii by a combined metabolomic and proteomic approach. Environ Pollut 255:113333

Yadetie F, Karlsen OA, Lanzén A, Berg K, Olsvik P, Hogstrand C, Goksøyr A (2013) Global transcriptome analysis of Atlantic cod (Gadus morhua) liver after in vivo methylmercury exposure suggests effects on energy metabolism pathways. Aquat Toxicol 126:314–325

Zhol S, Ackman RG, Morrison C (1995) Storage of lipids in the myosepta of Atlantic salmon (Salmo salar). Fish Physiol Biochem 14:171–178